Journal of Dental Research
DS1–DS5

DOI: 10.1177/0022034515576051
jdr.sagepub.com

Wnt5a/Ror2 Mediates Temporomandibular Joint Subchondral Bone Remodeling

T. Yang[1,2*], J. Zhang[1*], Y. Cao[3*], M. Zhang[1], L. Jing[1], K. Jiao[1], S. Yu[1], W. Chang[4], D. Chen[5], and M. Wang[1]

Appendix

Materials and Methods

Dental Operation of Unilateral Anterior Crossbite

The left pair of incisors was encased with small metal tubes using zinc phosphate cement. The maxillary and mandibular tubes were made from lactogenesis needles (inside diameter: 3 mm, length: 2.5 mm; ShinvaAnde, Shangdong, China) and syringe needles (inside diameter: 2 mm, length: 4.5 mm), respectively. The surface of the upper end of the mandibular tube was slanted at a 135-degree angle to the labial side to generate unilateral anterior crossbites (UACs) between the left incisors. The animals wore the dental prostheses for 4 wk before their mandibular condyles were removed and analyzed.

Analyses of Subchondral Trabecular Bone in TMJs by Micro–computed Tomography, Histology, and Immunohistochemistry

Temporomandibular joints (TMJs) were fixed and scanned by micro–computed tomography (μCT) to assess changes in bone mass and skeletal parameters as previously described (Glantschnig et al. 2011). Briefly, the TMJs of rats were scanned with an in vitro μCT system (eXplore Locus SP; GE, Fairfield, CT, USA) at 80 kV and 80 μA. The X-ray beam was reconstructed with an isotropic voxel size of 8 μm. Two 0.5 × 0.5 × 0.5-mm trabecular bones in the subchondral area from the central and posterior third part of TMJ condyles were selected for quantitative analysis. The bone volume to tissue volume (BV/TV, %), trabecular number (Tb.N), trabecular thickness (Tb.Th), and trabecular separation (Tb.Sp) were measured by the GE microview software.

TMJ samples were decalcified, embedded in paraffin, and sectioned (at 5-μm thickness) (Wang et al. 2014). The sections were stained with hematoxylin and eosin (H&E) according to the usual methods, and images were captured by a Leica DFC490 system (Leica, Solms, Hessen, Germany). Analyses were performed in 2 square frames (0.5 × 0.5 mm), which were located at the middle and posterior center of the subchondral trabecular bone under the osteochondral junction (Fig. 1C, black frames). BV/TV, Tb.Th, Tb.N, and Tb.Sp were measured as described previously (Zhang et al. 2013).

The sections were stained with tartrate-resistant acid phosphatase (TRAP; Sigma-Aldrich, St. Louis, MO, USA) according to the manufacturer's instructions to assess osteoclast numbers or subjected to immunohistochemical staining with an anti-osteocalcin (Ocn) antibody (1:200, sc-30044; Santa Cruz Biotechnology, Santa Cruz, CA, USA). The pre-immune–immunoglobulin G (IgG) (Solarbio, Beijing, China) with the same animal origin and work concentration as the primary antibody were used as negative control. TRAP-positive cells that contained 3 or more nuclei were considered osteoclasts. Bone images were captured by light microscopy. Regions from the osteochondral junction to 0.5 mm below were selected and analyzed histomorphometrically for the numbers (per millimeter bone surface) of TRAP-positive osteoclasts and Ocn-positive osteoblasts along the subchondral bone marrow cavity of the mandibular condyles by Photoshop CS4 software (Adobe, San Jose, CA, USA) by converting pixels to millimeters.

Phenotypic Analysis and Sorting of BMSCs by Flow Cytometry

Passage 4 rat bone marrow stromal cells (BMSCs) were incubated with PerCP-conjugated anti-CD34, FITC-conjugated anti-CD45 (Santa Cruz Biotechnology), PerCP-eFluor 710–conjugated anti-CD54 (eBioscience, San Diego, CA,

[1]State Key Laboratory of Military Stomatology, Department of Oral Anatomy and Physiology, School of Stomatology, the Fourth Military Medical University, Xi'an, Shaanxi, China
[2]Department of Stomatology, Chinese PLA General Hospital, Beijing, China
[3]Department of Cardiac Surgery, Air Force General Hospital, PLA, Beijing, China
[4]Endocrine Research Unit, Department of Veterans Affairs Medical Center, Department of Medicine, University of California, San Francisco, CA, USA
[5]Department of Biochemistry, Rush University Medical Center, Chicago, IL, USA
*Authors contributing equally to this article.

Corresponding Author:
M. Wang, State Key Laboratory of Military Stomatology, Department of Oral Anatomy and Physiology, School of Stomatology, the Fourth Military Medical University, Xi'an, 710032, China.
Email: mqwang@fmmu.edu.cn

Appendix Table. Primer Sequences of Real-time Polymerase Chain Reaction.

Gene Name	Species	Forward Primer (5′ to 3′)	Reverse Primer (5′ to 3′)
Gapdh	Rat	GGCACAGTCAAGGCTGAGAATG	ATGGTGGTGAAGACGCCAGTA
Rankl	Rat	GCAGCATCGCTCTGTTCCTGTA	GCATGAGTCAGGTAGTGCTTCTGTG
Opg	Rat	CTCATCAGTTGGTGGGAATGAAGA	ACCTGGCAGCTTTGCACAATTA
Rank	Rat	GAAGCACACCAAGGGACGA	CTACCACAGAGATGAAGAGGAGCA
CatK	Rat	CGGCTATATGACCACTGCCTTC	TTTGCCGTGGCGTTATACATACA
Trap	Rat	GTGCATGACGCCAATGACAAG	TTTCCAGCCAGCACGTACCA
Runx2	Rat	CATGGCCGGGAATGATGAG	TGTGAAGACCGTTATGGTCAAAGTG
Ocn	Rat	AAGGTGGTGAATAGACTCCG	AAACGGTGGTGCCATAGATG
Osx	Rat	CACCCATTGCCAGTAATCTTCGT	GGACTGGAGCCATAGTGAGCTTC
Alp	Rat	CACGTTGACTGTGGTTACTGCTGA	CCTTGTAACCAGGCCCGTTG
Cxcr4	Rat	AGTGACCCTCTGAGGCGTTTG	GAAGCAGGGTTCCTTGTTGGAGT
M-CSF	Rat	GACAGGTGGAACTGCCAGTGTAGA	GGTAGTGGTGGACGTTGCCATA
Wnt5a	Rat	ACTTGCACAACAATGAAGCAGGTC	CAGCCAGCATGTCTTGAGGCTA
Ror2	Rat	TTGGGAACCGAACTATTTATGTGGA	CAAACTGCGAGCACTGGTCTG
Gapdh	Mouse	ATGGTGGTGAAGACGCCAGTA	GGCACAGTCAAGGCTGAGAATG
Ror2	Mouse	CATTGGGAACCGGACTATTTATGTG	CTGGTCTGACAGTTGCGTGGA
Cxcl12	Mouse	CAGAGCCAACGTCAAGCATC	TTAATTTCGGGTCAATGCACAC
Runx2	Mouse	GATGAGCGACGTGAGCC	ATGGTGCGGTTGTCGTG
Rankl	Mouse	GCATCGCTCTGTTCCTGT	AGGCTTGTTTCATCCTCC
Opg	Mouse	AGACGCACCTAGCACTGAC	CCAGGAGCACATTTGTCAC

USA), and PE-conjugated anti–rat CD90 (BioLegend, San Diego, CA) antibodies (1 μg/10^6 cells), respectively, at 4 °C for 1 h in the dark. Aliquots of 10,000 cells were analyzed by fluorescence-activated cell sorting (FACS) with a BD FACSAria flow cytometer (BD Biosciences, San Jose, CA, USA).

To assess the percentage of BMSCs to TMJ subchondral bone marrow cells, bone marrow cells were isolated from TMJ subchondral bone between the osteochondral junction and the condyle's sigmoid notch and stained with PerCP-conjugated anti-CD34, FITC-conjugated anti-CD45, and PE-conjugated anti–rat CD90 antibodies (1 μg/10^6 cells) simultaneously at 4 °C for 1 h after erythrocytes were lysed with BD FACS Lysing Solution (BD Biosciences) to obtain the number of $CD34^-$, $CD45^-$, and $CD90^+$ BMSCs by FACS.

Total RNA Extraction and Real-time PCR

Total RNA was isolated by Trizol (Invitrogen, Carlsbad, CA, USA) and reverse-transcribed into complementary DNA (cDNA) by a PrimeScript RT reagent Kit Perfect Real Time (TaKaRa Biotechnology, Dalian, China). Real-time PCR was performed using SYBR® Premix Ex TagTMII (TaKaRa) with an ABI 7500 real-time polymerase chain reaction (PCR) system (Applied Biosystems, Foster, CA, USA) at the manufacturer's recommended conditions. The relative expression levels were calculated using the comparative threshold cycle (ΔCT) method. All primer sequences are shown in the Appendix Table.

Western Blot Assays

BMSCs were lysed with RIPA lysis buffer (Beyotime Institute of Biotechnology, Jiangsu, China) containing PMAS phosphatase inhibitors (Beyotime). Total protein lysates were separated by sodium dodecyl sulfate polyacrylamide gel electrophoresis (SDS-PAGE), transferred to an NC (Bio-Rad Laboratories, Hercules, CA, USA) membrane, analyzed with SDF-1 antibody (Santa Cruz Biotechnology) or Wnt5a antibody (Abcam, Cambridge, UK), and visualized by Immobilon Western Chemiluminescent HRP Substrate (Millipore, Billerica, MA, USA).

MTT Assays

In methyl-thiazolyl-tetrazolium (MTT) assays, BMSCs were seeded in 96-well plates at a density of 2,000 cells/well and incubated with 20 μL MTT (5 mg/mL; Sigma-Aldrich) for 4 h. The supernatant was aspirated and the formazan was dissolved in 150 μL DMSO. The absorbance was measured at 490 nm using a Synergy HT multidetection microplate reader (Bio-Tek, Winooski, VT, USA).

Cell Cycle Analysis

BMSCs were stored in 70% ethanol (in phosphate-buffered saline [PBS]) at 4 °C overnight. Cells were stained with 100 mg/mL propidium iodide (Sigma-Aldrich) at 4 °C for 30 min and then analyzed using a BD FACSAria flow cytometer (BD Biosciences).

CFU-F Assays

BMSCs (400 cells/well) were seeded in 6-well plates, cultured for 3 wk, and stained with 0.16% Giemsa stain solution. Colonies larger than 1 mm^2 were counted.

Knockdown of Ror2 *Expression by Small Interfering RNA (siRNA)*

CL-BMSCs (5×10^4 cells/well in 24-well plates) were incubated with each of the 2 mice *Ror2* siRNAs (20 pmol/5×10^4 cells; siRNA-795, ACCGGACUAUUUAUGUGGATT-UCCA

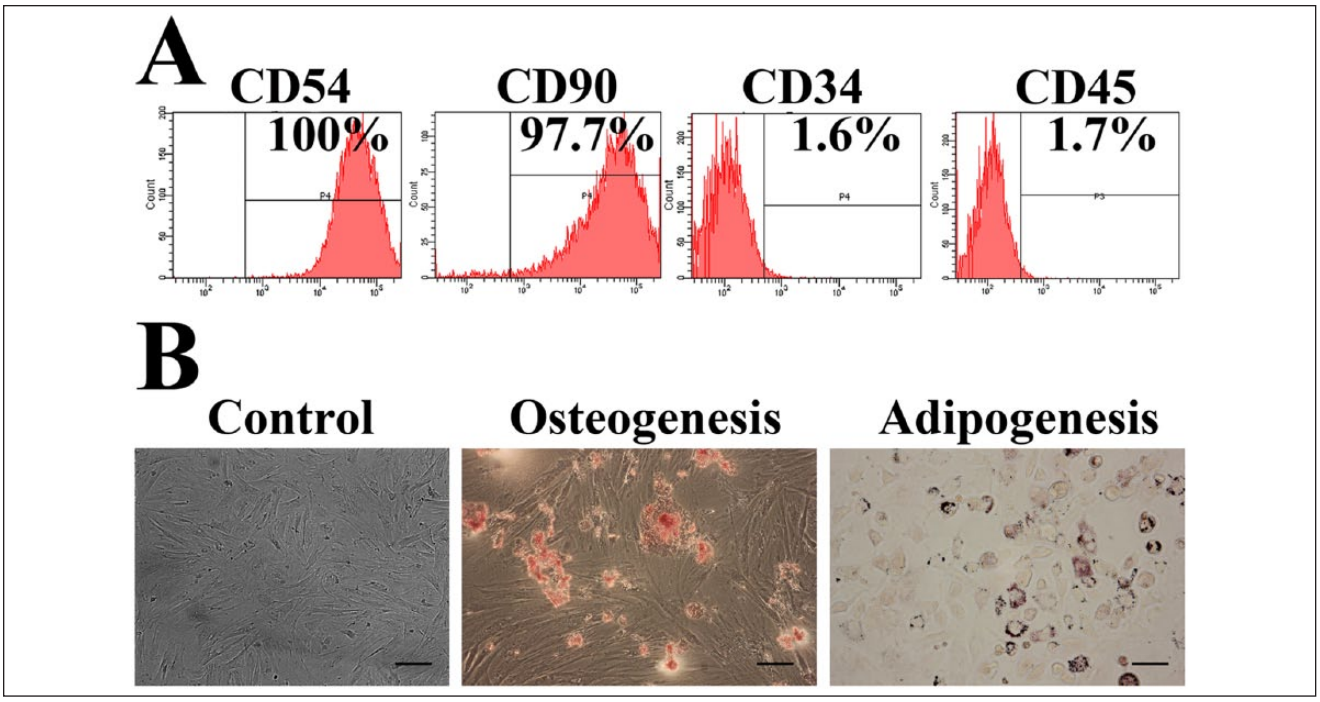

Appendix Figure 1. Pluripotency of bone marrow stromal cells (BMSCs) from subchondral bone of mandibular condyles in vitro. (**A**) Peak chart for the cells detected with anti-CD34, anti-CD45, anti-CD54, and anti-CD90 by flow cytometry. (**B**) Osteogenic and adipogenic potentials of the cells were assessed by Alizarin red and Oil red O staining as described in Methods. Bars = 40 μm.

CAUAAAUAGUCCGGUTT; siRNA-2477, GGGCAACC UAUCCAACUAUTT-AUAGUUGGAUAGG UUGCCCTT; GenePharma, Shanghai, China) or control siRNA (UUCUCCG AACGUGUCACGUTT-ACGUGACACGUUCGGAG AATT) for 6 h and used for the following assays 48 h later.

UAC-treated BMSCs (5×10^4 cells/well in 24-well plates) were incubated with each of the 3 rat *Ror2* siRNAs (20 pmol/5×10^4cells; siRNA-1131, GUCGCUAUCACCAGUGUUATT-UAACACUGGUGAUAGCGACTT; siRNA-1324, GUGGU G C U U U A C G C A G A A U T T - A U U C U G C G U A AAGCACCACTT; siRNA-2124, CCGCCGAUUACUA C A A A C U T T - A G U U U G U A G U A A U C G G C G G T T; GenePharma) or control siRNA (UUCUCCGAACGUGU CACGUTT-ACGUGACACGUUCGGAGAATT) for 6 h and used for the cell migration and co-culture assays 48 h later.

Cell Differentiation Assays

To induce osteoblast differentiation, the isolated BMSCs or CL-BMSCs with or without knockdown of *Ror2* expression were cultured in α–minimum essential medium (MEM) supplemented with 10% fetal bovine serum (FBS), 5 mM L-glycerophosphate (Sigma-Aldrich), 100 nM dexamethasone (MP Biomedicals, Santa Ana, CA, USA), and 50 mg/mL ascorbic acid (Sigma-Aldrich) for 2 wk. Matrix mineralization was evaluated by Alizarin red (0.1%, wt/vol) staining at 37 °C for 30 min. After 3 washes with PBS, mineral stains were solubilized by cetylpyridinium chloride (100 mM) and quantified by absorbance at 570 nm using a Synergy HT multidetection microplate reader (Bio-Tek). In some experiments, CL-BMSCs were treated with Wnt5a (200 ng/mL; R&D Systems, Minneapolis, MN, USA), JNK inhibitor SP600125 (10 μM; Sigma-Aldrich), or Ca^{2+}/NFAT inhibitor cyclosporine

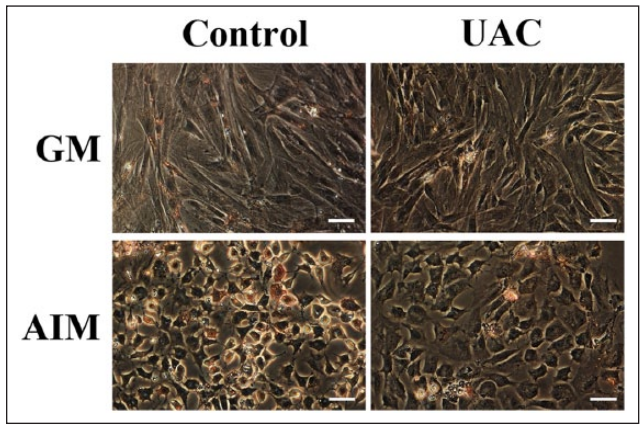

Appendix Figure 2. Adipogenic differentiation of bone marrow stromal cells (BMSCs) isolated from subchondral bone of mandibular condyles of control (Con) and unilateral anterior crossbite (UAC)–treated rats. Oil red O staining was performed after BMSCs were cultured in adipogenic induction medium (AIM) or growth medium (GM) for 3 wk to identify lipid vesicles (in red). Bars = 40 μm.

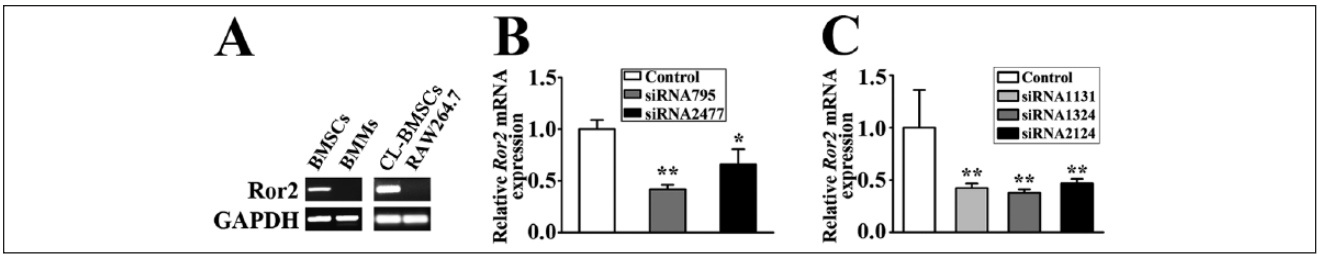

Appendix Figure 3. *Ror2* small interfering RNA (siRNA) knocked down *Ror2* expression in the bone marrow stromal cell line (CL-BMSCs) and unilateral anterior crossbite (UAC)–treated BMSCs. (**A**) Agarose gel electrophoresis analysis of *Ror2* complementary DNA (cDNA) amplified by polymerase chain reaction (PCR) from RNAs extracted from rat BMSCs, rat bone marrow macrophages (BMMs), CL-BMSCs, and RAW264.7 cells. These data show *Ror2* expression in the rat BMSCs and CL-BMSCs but not in BMMs and RAW264.7 cells. (**B**) Quantitative PCR analyses of RNAs extracted from CL-BMSCs preincubated with control siRNA or 2 different *Ror2* siRNAs to knock down *Ror2* expression. Power = 0.72, 0.63 (siRNA795 and siRNA2477 vs. control, respectively). (**C**) Quantitative PCR analyses of RNAs extracted from UAC-treated BMSCs preincubated with control siRNA or 3 different *Ror2* siRNAs to knockdown *Ror2* expression. Power = 0.55, 0.56, 0.53 (siRNA1131, siRNA1324, and siRNA2124 vs. control, respectively). Data are presented as means ± SD. **P* < 0.05. ***P* < 0.01.

A (1 μM; Enzo Life Science, Farmingdale, NY, USA) for 2 wk after the cells were replated for 24 h.

To assess the adipogenic potential of rat BMSCs, BMSCs were cultured with α-MEM supplemented with 10% FBS, 10 nM indometacin (MP Biomedicals), 10 nM dexamethasone (MP Biomedicals), 0.5 mM isobutylmethylxanthine (IBMX; MP Biomedicals), and 2 mM insulin (Sigma-Aldrich) for 3 wk. Lipid accumulation was stained by Oil red O (0.3%, wt/vol) for 20 min at room temperature.

Cell Migration Assay

To study the migration of BMSCs toward bone matrices, TMJ subchondral bone fragments between the osteochondral junction and the simoid notch and 2×10^3 BMSCs were seeded into the lower and upper compartments of transwell chambers (24-well format; Corning, Corning, NY, USA), respectively. The 2 compartments were separated by a perforated membrane with 8-μm pores. After 24 h, BMSCs that migrated across the transwell membrane were stained with DAPI nuclear dye. Ten fields at 200× magnification were selected randomly, and cell counts from the fields were averaged.

To assess the migration of osteoclast precursors toward BMSCs, serum-deprived BMSCs or CL-BMSCs (2.5×10^4/well) and osteoclast precursors (4×10^3/well) were added to the lower and upper compartments of 24-well transwell plates in a 24-h interval, respectively, and cultured for 24 h. The transwell membranes with 3-μm pores were used for BMMs (NUNC, Thermo, Waltham, MA, USA), and those with 8-μm pores were used for RAW264.7 cells (Corning). Cells migrating across the transwell membrane were stained with DAPI and counted. In some experiments, UAC-treated BMSCs were treated with CXCR4 antagonist AMD3100 (1 μg/mL; Abcam), and CL-BMSCs in the lower compartments were treated with Wnt5a (400 ng/mL), JNK inhibitor SP600125 (10 μM), or Ca^{2+}/NFAT inhibitor cyclosporine A (1 μM) 24 h after the cells were seeded.

Terminal Deoxynucleotidyl Transferase dUTP Nick End Labeling (TUNEL) Staining

To determine osteoclast precursors apoptosis, terminal deoxynucleotidyl transferase dUTP nick end labeling (TUNEL) staining was performed using an in situ cell death detection kit, fluorescein (Roche Life Science, Indianapolis, IN, USA) according to the manufacturer's instructions. Briefly, after treating RAW264.7 cells with 10 μM SP600125 for 7 d, cells were fixed with 4% paraformaldehyde (Sigma-Aldrich) at 4 °C for 20 min, exposed to 0.1% Triton X-100 (in 0.1% sodium citrate) for 2 min on ice, and incubated with TUNEL reaction mixture at 37 °C for 60 min in the dark. Images were captured by an Olympus inverted microscope system (Olympus, Tokyo, Japan), and the numbers of TUNEL-positive cells per 200× field were counted.

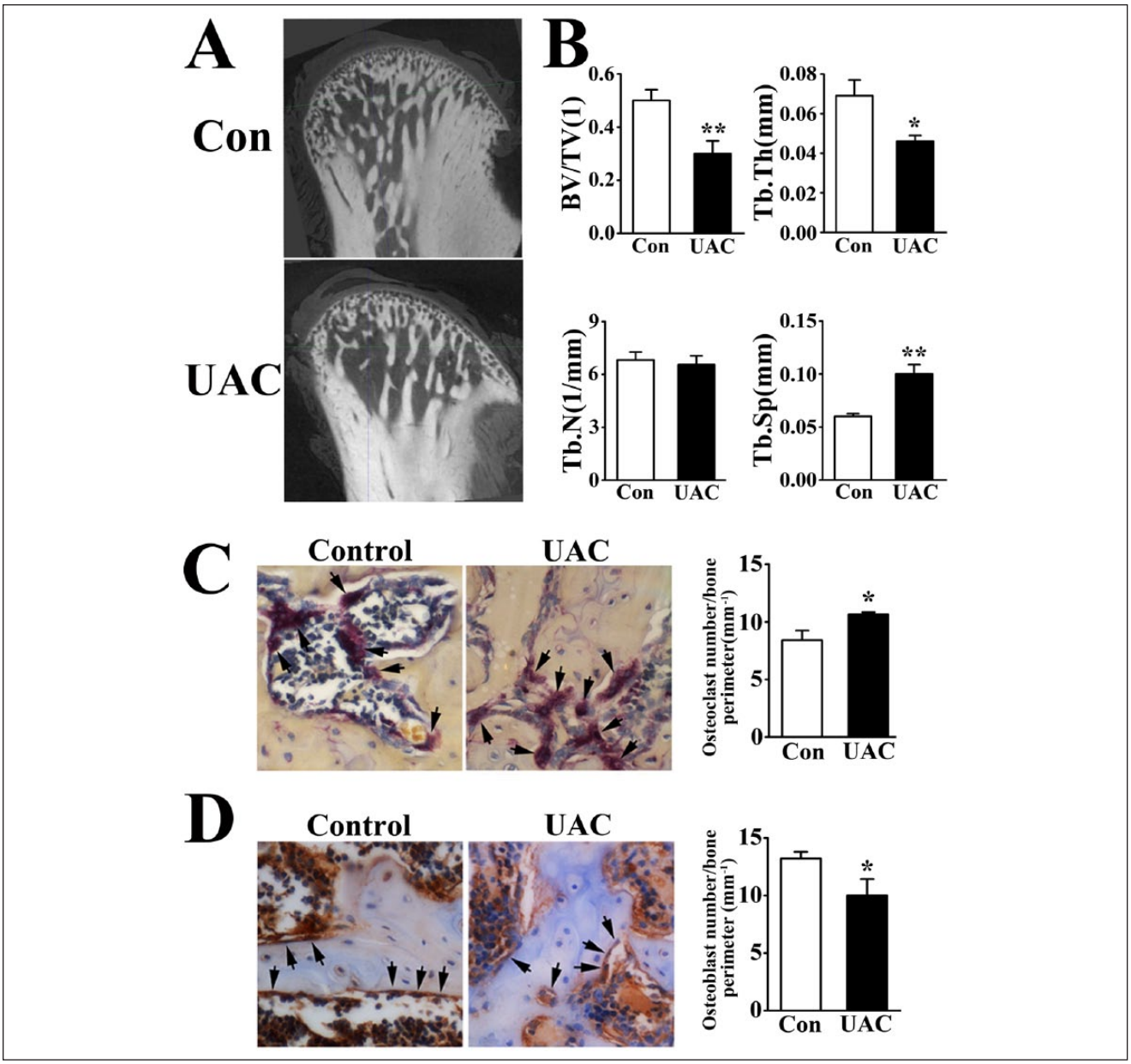

Appendix Figure 4. Unilateral anterior crossbite (UAC) induced subchondral trabecular bone loss with increased osteoclast number but decreased osteoblast number in temporomandibular joints (TMJs) at 8 wk. (**A**) Micro–computed tomography (CT) images and (**B**) quantifications of subchondral trabecular bone parameters in control and UAC-treated TMJs 8 wk after operation. Power = 0.87 (BV/TV), 0.82 (Tb.Th), and 0.88 (Tb. Sp). (**C**) Tartrate-resistant acid phosphatase (TRAP)–positive multinucleated osteoclasts (black arrow) and their numbers per bone surface (mm^{-1}) (in histogram) in the TMJ subchondral trabecular bone at 8 wk. Bars = 50 μm. Power = 0.64. (**D**) Ocn-positive osteoblasts (black arrow) and their numbers per bone surface (mm^{-1}) (in histogram). Bars = 50 μm. Power = 0.61. Data are presented as means ± SD. **P* < 0.05. ***P* < 0.01.

Appendix References

Glantschnig H, Scott K, Hampton R, Wei N, McCracken P, Nantermet P, Zhao JZ, Vitelli S, Huang L, Haytko P, et al. 2011. A rate-limiting role for Dickkopf-1 in bone formation and the remediation of bone loss in mouse and primate models of postmenopausal osteoporosis by an experimental therapeutic antibody. J Pharmacol Exp Ther. 338(2):568–578.

Wang YL, Zhang J, Zhang M, Lu L, Wang X, Guo M, Zhang X, Wang MQ. 2014. Cartilage degradation in temporomandibular joint induced by unilateral anterior crossbite prosthesis. Oral Dis. 20(3):301–306.

Zhang J, Jiao K, Zhang M, Zhou T, Liu XD, Yu SB, Lu L, Jing L, Yang T, Zhang Y, et al. 2013. Occlusal effects on longitudinal bone alterations of the temporomandibular joint. J Dent Res. 92(3):253–259.